Large-amplitude quantum fluctuations and subgap optical absorption in *trans*-polyacetylene

Assa Auerbach* and S. Kivelson
Department of Physics, State University of New York, Stony Brook, New York 11794-3800
(Received 27 December 1985)

We show that in the frequency regime of the subgap tail, large-amplitude fluctuations of the $(CH)_x$ chain are involved in the optical absorption process. A recently developed semiclassical technique is applied to calculate the absolute absorption coefficient which is related to multidimensional tunneling of soliton pairs. We include the renormalization effects of weak electron-electron interactions and background transverse phonons. Good agreement with recent experimental data is found. Experimental predictions are made concerning the isotope dependence and the effect of the soliton shape mode on the absorption coefficient.

I. INTRODUCTION

The main features of the optical properties of polyacetylene $(CH)_x$ have been successfully explained by theories based on the model Hamiltonian of Su, Schrieffer, and Heeger (SSH).[1,2] Most studies of this model have treated the lattice in the classical ("static") approximation; quantum fluctuations of the lattice have thus been ignored. In this approximation the ground state consists of a dimerized chain (alternating long and short bonds), and hence a gap of energy $2\Delta_0 = 1.4-1.8$ eV in the electronic spectrum. The resulting optical absorption coefficient $\alpha(\omega)$ was calculated by SSH; it exhibits an unphysical inverse-square-root divergence at threshold $\alpha(\omega) \sim (\hbar\omega - 2\Delta_0)^{-1/2}$ due to the one-dimensional density of electronic states. Inclusion of any of a number of other interactions which were not included in the simple treatment of SSH will suppress this divergence: Lee and Kivelson[3] have shown that local-field effects produced by the three-dimensional screening of the electromagnetic field eliminate this divergence. The presence of interchain electron hopping[3] makes the electronic band structure three dimensional ($4t_\perp$ is the interchain bandwidth), and hence also removes the band-edge singularity and slightly shifts the threshold energy to $2(\Delta_0 - t_\perp)$. However, these modifications still cannot properly account for the experimentally observed exponentially falling tail of the optical absorption which extends deep into the gap, down to at least $\hbar\omega = 1.1$ eV (see Fig. 1.). Among the experiments which are sensitive to this tail are the measurements of photothermal deflection spectroscopy (PDS) of Weinberger *et al.*,[4] which measure the absolute absorption rate; measurements of photoinduced absorption (Blanchet *et al.*[5]); and measurements of photoconductivity (Laughlan *et al.*[6]), which measure the rate of photoproduction of charged solitons.

The tail structure is observed most clearly in the most carefully prepared samples of pristine *trans*-$(CH)_x$, which suggests that the relevant broadening mechanism is not related to static disorder. We therefore suggest that the quantum fluctuations of the lattice, which were frozen out in the classical approximation, are crucial in determining the photoresponse functions of $(CH)_x$.

To get a feeling for whether this suggestion is plausible, let us, as a first crude approximation, imagine treating the ion's zero-point motion as a form of quenched disorder which produces a Gaussian white-noise random potential for the electrons. In this approximation, we can easily compute the density of states in the valence and conduc-

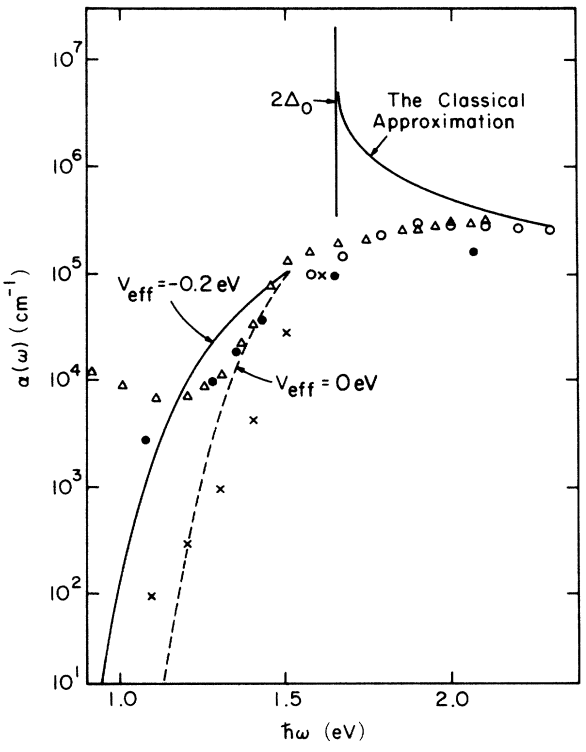

FIG. 1. Optical absorption coefficient of *trans*-$(CH)_x$. The following data is given in absolute units: *x*-(NH_3) compensated sample, Ref. 4; and ○, Ref. 5. In relative units: △, the uncompensated 0.5 film of Ref. 4. ● is the photoinduced change in transmission at 1370 cm^{-1}, Ref. 5. The right solid line is the result of the static approximation [Eq. (2.6)], and the present calculation [Eq. (4.9)] is given by the left lines for two different values of the average soliton creation energies V_{eff}.

tion band using the method of Halperin.[7] We can estimate the magnitude of the random potential felt by the electrons using the Bogoliubov–de Gennes equation[8] and computing the mean-square fluctuations of the order parameter in the ground state. This has been done by Hicks and Blaisdell,[9] who find that $\langle \delta\Delta^2 \rangle = 0.42\Delta_0^2$; this implies a root-mean-squared disorder potential $\Delta_1 = 0.48$ eV. If taken seriously, this would imply such a broad absorption tail that there would be no observable optical threshold energy at all.[10]

However, the quenched disorder model is applicable, at best, when the magnitude of the lattice fluctuations is small, since otherwise the lattice dynamics are strongly influenced by the induced changes in the electronic spectrum, especially of the localized states. We can, however, conclude from this argument that quantum fluctuations of the lattice will have a large effect on the optical absorption.

Sethna and Kivelson[11] (SK) have shown that at low energies the only electronic states participating in the optical absorption process are the even and odd parity localized states associated with a virtual soliton-antisoliton pair, which are formed by a large-amplitude, localized lattice fluctuation. SK treated the valence electrons as adiabatic slaves of the lattice motion. Within this approximation, the effective lattice dynamics are determined by the two adiabatic potential energies corresponding, respectively, to the instantaneous electronic ground state and the first excited (exciton) states. SK then mapped the resulting two-level transition rate problem onto an equivalent multidimensional tunneling calculation which is amenable to the solution using the instanton bounce formalism of Callan and Coleman.[12] SK estimated $\ln[\alpha(\omega)]$ to leading order in $\hbar$ using an approximate solution to the classical dynamics. They found good agreement with the photoconductivity data of Lauchlan *et al.* However, the absolute absorption coefficient was not determined since the prefactor expression of the bounce is difficult to evaluate.

Later, Su and Lu[13] used a nonradiative decay approach to compute $\alpha(\omega)$. Their treatment is simpler than the instanton approach, but it implicitly ignores the extremely anharmonic nature of the large-amplitude lattice fluctuations. Although their results are similar in spirit to those obtained by SK, their method is inadequate for obtaining the asymptotic behavior of $\alpha(\omega)$ near threshold.

The more recent experiments of Refs. 4 and 5, which are in good qualitative agreement with the SK results, demonstrate the need to complete the calculation and obtain quantitatively reliable results. In this paper we begin by rederiving the results of SK using a correlation function approach, and then calculate the absorption coefficient by applying a newly developed technique called the path decomposition expansion (PDX).[14,15] This method enables us to use separate approximation schemes in the different parts of configuration space and to evaluate the Green functions in the classically forbidden region to leading order in $(\hbar\omega_0/\Delta_0)$, the dimensionless quantum parameter, where $\hbar\omega_0$ is the long-wavelength optical phonon frequency of the dimerized lattice. Since the PDX is discussed at length in Ref. 15, we will refer the reader there for detailed derivations of some of the more technical details of the approach.

We are able to incorporate three additional effects in this calculation which have not been treated previously.

(1) Quantum corrections to the lattice potential energies due to soliton-induced shifts in the phonon spectrum.

(2) Electron-electron (e-e) interactions [using the perturbative calculations of Wu and Kivelson[16] (WK)].

(3) The modulation of the absorption spectrum caused by excitation of the symmetric width oscillation mode of the final soliton pair. This is a "backscattering" effect that is, in principle, missed by the bounce method.[14] It has not been observed previously, but it should be experimentally detectable, and its observation would provide strong additional evidence of the subgap soliton-pair production.

II. THE SSH MODEL AND THE OPTICAL ABSORPTION COEFFICIENT

The SSH Hamiltonian for a single chain of *trans*-$(CH)_x$ is

$$H_{\rm SSH} = H_{\rm el} + H_{\rm lat} ,$$

$$H_{\rm el} = -t_0 \sum_{ns} [1 + \tfrac{1}{4}(-1)^n(\Delta_n + \Delta_{n+1})] \times (c_{ns}^{\dagger} c_{(n+1)s} + \text{H.c.}) , \tag{2.1}$$

$$H_{\rm lat} = [1/(4\alpha)^2] \left[\tfrac{1}{2} \sum_n (P_n)^2/M + \tfrac{1}{2} K \sum_n (\Delta_n + \Delta_{n+1})^2 \right] ,$$

where $c_{ns}^{\dagger}$ creates an electron of spin s at site n; Δ_n is the staggered order parameter ("dimerization"); P_n is the momentum conjugate to Δ_n; and $4t_0$, M, K, and α are, respectively, the C_n bandwidth, the mass of the CH group, the bare stiffness constant, and the electron-phonon coupling constant. The continuum version of this model is known as the Takayama, Lin-Liu, and Maki; (TLM) model:[8]

$$H_{\rm TLM} = \sum_s \int dx\, \psi_S(x) \left[-i v_F \sigma_z \frac{\partial}{\partial x} + \Delta(x)\sigma_x \right] \psi_S(x) + 2/g^2 \int dx (\tfrac{1}{2}\Delta^2 + \tfrac{1}{2}\omega_Q^2 \Delta^2) , \tag{2.2}$$

where $v_F = 2t_0 a/\hbar$, $g^2 = \hbar\pi v_F \omega_Q^2 \lambda$, $\lambda = (4\alpha)^2/4\pi t_0 K$, a is the lattice constant, and the bare optical-phonon frequency is $\omega_Q^2 = 4K/M$. The field is defined as $\Delta(na) = \Delta_n$, and $\psi_S(x)$ is a two-component fermion field. In the classical approximation, both models have doubly-degenerate broken-symmetry ground states with the dimerization $\langle \Delta \rangle = \pm\Delta_0$. The corresponding electronic spectrum has a gap $2\Delta_0$ between the valence and conduction bands. For pristine $(CH)_x$ the Fermi energy lies exactly in the midgap. Since the band gap is much smaller than the bandwidth, calculations which involve only states with energies of order $2\Delta_0$ or smaller can be done using the two models interchangeably. WK showed that the effects of weak e-e interactions can be accounted for using pertur-

bation theory. We shall therefore begin by ignoring these interactions for simplicity's sake, and shall later correct the results to include their effect.

The optical absorption coefficient $\alpha(\omega)$ is determined from the dielectric function:

$$\epsilon(\omega)=\epsilon_\infty+(4\pi/3)(e^2/\xi_0\Delta_0)(na\xi_0^2)S(\omega)\ , \tag{2.3}$$

where $S(\omega)$ is the following electronic correlation function:

$$S(\omega)=-i(\Delta_0/\hbar\xi_0 L)\int_0^\infty dt\, e^{i\omega t}\langle x(t)x(0)\rangle$$
$$=(\Delta_0/L\xi_0)\sum_\beta \frac{|\langle\psi_0|x|\psi_\beta\rangle|^2}{(E_\beta-E_0-\hbar\omega+i\delta)}\ . \tag{2.4}$$

$\epsilon_\infty\approx 3$ is the high-frequency dielectric constant which includes the effects of the σ electrons (and is pure real), $\xi_0=\hbar v_F/\Delta_0$ is the electronic correlation length, n is the volume density of (CH) monomers, ψ_β are the many-body electron-phonon wave functions, and x is the electron dipole operator. We have chosen to normalize S in such a way that it is finite in the thermodynamic limit ($L\to\infty$) and in the continuum limit (ξ_0/a and $t_0/\Delta_0\to\infty$ with na, ξ_0, and Δ_0 held constant). The optical absorption coefficient is then

$$\alpha(\omega)=(\omega/\sqrt{2}c)\sqrt{|\epsilon|-\epsilon'}\approx(\omega/2c)\frac{\epsilon''}{\sqrt{\epsilon'}}$$
$$=\alpha_0\left[\frac{\hbar\omega}{\Delta_0}\right]S''(\omega)\ , \tag{2.5a}$$

where

$$\alpha_0=\tfrac{1}{3}na(2\pi/\sqrt{\epsilon'})(e^2/\hbar c)\approx 2\times 10^5\ \mathrm{cm}^{-1} \tag{2.5b}$$

and prime and double prime denote the real and imaginary parts, respectively. The factor of $\frac{1}{3}$ was obtained by averaging over the directions of the polarization vector. Note that since ϵ' is a slowly varying function of ω, the frequency dependence of $\alpha(\omega)$ derives predominantly from S'', and hence depends only on the properties of the state with energy $\hbar\omega$ above the ground state.

To implement the adiabatic approximation, it is convenient to express the full wave function ψ_β in terms of the electronic eigenstates χ_j in the presence of the instantaneous static lattice configuration Δ. χ_j depends parametrically on Δ:

$$\psi_\beta=\sum_j \phi_\beta^j\chi_j\ ,$$

where $\phi_\beta^j[\Delta]$ is a wave functional of the lattice configuration Δ. In the classical or static approximation, fluctuations of Δ about its most probable value $[\Delta(x)=\Delta_0]$ are ignored, which amounts to approximating ϕ_β^j by a δ functional. The resulting expression for $\alpha(\omega)$ was evaluated by SSH, and by Suzuki *et al.*:[17]

$$\alpha(\omega)=16\alpha_0(2\Delta_0/\hbar\omega)^2[(\hbar\omega/2\Delta_0)^2-1]^{-1/2}\ . \tag{2.6}$$

We plot this expression in Fig. 1 and compare it to the experimental data. It is clear that the classical approximation is only valid for $\hbar\omega\gg 2\Delta_0$. We now consider $\hbar\omega\lesssim 2\Delta_0$. In the adiabatic approximation, the lattice wave functions satisfy the effective Schrödinger equation:

$$\left[-\frac{\hbar^2(4\alpha)^2}{2M}\sum_n\frac{\partial^2}{\partial\Delta_n^2}+V_j[\Delta]\right]\phi_\beta^j=E_\beta^j\phi_\beta^j\ . \tag{2.7a}$$

$\epsilon_j[\Delta]$ is the adiabatic potential energy corresponding to electronic state j,

$$V_j[\Delta]=\epsilon_j[\Delta]+\tfrac{1}{2}K/(4\alpha)^2\sum_n(\Delta_n+\Delta_{n+1})^2\ , \tag{2.7b}$$

and $\epsilon_j[\Delta]$ is the instantaneous electronic energy of state χ_j. The adiabatic approximation is valid at least so long as $h=\hbar\omega_0/|\epsilon_i-\epsilon_j|\ll 1$, where ω_0 is the $k=0$ optical phonon frequency. For the present purposes, it is necessary to keep track of only the electronic ground state, $j=0$, and the first excited singlet state, $j=1$; higher lying electronic states only become important when $\hbar\omega>2\Delta_0$. We shall see that h is also the appropriate dimensionless measure of the magnitude of $\hbar$ which enters the semiclassical approximation for the lattice wave functions: both the adiabatic and semiclassical approximations are asymptotic expansions in small h. Having decided only to include transitions between the two lowest electronic states, we can easily obtain a spectral representation for S in Eqs. (2.5) in terms of lattice wave functions alone:

$$S(\omega)=\frac{\Delta_0}{L\xi_0\hbar}\int\mathscr{D}\Delta\,\mathscr{D}\Delta'\{\phi_0^0[\Delta]\phi_0^0[\Delta']X_{01}[\Delta]X_{10}[\Delta']$$
$$\times G_1(\Delta,\Delta';\hbar\omega)\}\ , \tag{2.9}$$

where the integrals $\mathscr{D}\Delta=\prod_n d\Delta_n$ run over all lattice configurations Δ and Δ', X_{01} is the electronic dipole matrix element

$$X_{01}[\Delta]=\langle\chi_0|x|\chi_1\rangle \tag{2.10}$$

which depends parametrically on Δ, and G_1 is the lattice propagator in electronic state 1:

$$G_1(\Delta,\Delta';E)=-\hbar\sum_\beta\frac{\phi_\beta^1[\Delta]^*\phi_\beta^1[\Delta']}{(E-E_\beta^1+E_0-i\delta)}\ . \tag{2.11}$$

Since the lattice wave functions are highly peaked in the vicinity of the perfectly dimerized configuration, $\Delta(x)=\Delta_0$, all the configurations that make important contributions to S must have $\Delta(x)$ near Δ_0 except in a small (spatially localized) "defect" region. The presence of such a defect alters most of the electronic spectrum weakly, and pulls two or more localized states out of the continuum into the gap. The charge conjugation symmetry of the model implies that the localized states are placed at energies $\epsilon_0=-\epsilon_1$ placed symmetrically about midgap ($E_F=0$). If the lattice were truly static, an electronic transition could only occur when $\epsilon_1-\epsilon_0=\hbar\omega$. However, since the lattice configuration is merely a result of the quantum zero-point fluctuations of the lattice, the transition is necessarily virtual unless $\hbar\omega$ is greater than the total energy of the final-state continuum. $V_1(\Delta)$ takes on its minimum value of twice the soliton creation energy $2E_S=(4/\pi)\Delta_0$ when the lattice configuration corresponds to a far separated soliton pair. Thus there exists a threshold energy of $\hbar\omega\approx 2E_S$ for optical absorption.

For a given value of $\hbar\omega=\epsilon_1-\epsilon_0$, the lattice configura-

tion which minimizes the total adiabatic potential energy is[18]

$$\Delta_{S\bar{S}}(x;Y,R,K,A)=\Delta_0(1-A\{\tanh[K(x+\tfrac{1}{2}R-Y)] -\tanh[K(x-\tfrac{1}{2}R-Y)]\}) , \tag{2.12}$$

where K and A are the implicit functions of R,

$$K=A=\tanh(KR) , \tag{2.13}$$

and the value of R itself depends on $\hbar\omega$ according to the relation

$$R=\mathrm{sech}^{-1}(\hbar\omega/\Delta_0) . \tag{2.14}$$

We can think of $\Delta_{S\bar{S}}(x;Y,R,K,A)$ as being a soliton-antisoliton pair with center of mass Y and separation R where each soliton has a width K^{-1}. In the next section we shall see that R, Y, and K are natural collective coordinates. Crudely, $\Delta_{S\bar{S}}$ is the most probable lattice fluctuation that permits an electronic transition with energy $\hbar\omega$. Thus we expect the integrals in Eq. (2.9) to be dominated by lattice configurations Δ and Δ' near $\Delta_{S\bar{S}}$.

In the next section we will evaluate the integral Eq. (2.9) by the method of steepest descents (i.e., in the semiclassical approximation). However, this cannot be done directly since, due to the translational symmetry of the model, any saddle-point configuration $\Delta_f(\Delta_f\approx\Delta_{S\bar{S}})$ has a zero mode $u_0(x)$ associated with it such that the integrand is invariant under

$$\Delta_f(x)\to\Delta_f(x+dY)=\Delta_f(x)+dY\,\Delta_f'(x) =\Delta_f(x)+dY||\Delta_f'||u_0(x) , \tag{2.15}$$

where dY is an infinitesimal translation and

$$||\Delta_f'||=\int\frac{dx}{a}\,|\Delta_f'(x)|^2 . \tag{2.16}$$

We must therefore perform the integration over Y explicitly by changing the integration variables:

$$\mathcal{D}\Delta=\tilde{\mathcal{D}}\Delta\,dY\,||\Delta_f'||/\sqrt{\pi} , \tag{2.17}$$

where $\mathcal{D}\Delta$ represents the integral over all transverse configurations obeying

$$\int\frac{dx}{a}\Delta_f'(x)[\Delta(x)-\Delta_f(x)]=0 .$$

We can now formally do the Y integrals. At the same time, we shift integration variables to express the integrand in terms of fluctuations about Δ_f: $\Delta\to\Delta-\Delta_f$. The result is

$$S(\omega)=||\Delta_f'||^2\pi^{-1}(\Delta_0/\xi_0\hbar)\mathcal{S}(\omega) , \tag{2.18}$$

where

$$\mathcal{S}(\omega)=\int\tilde{\mathcal{D}}\Delta\tilde{\mathcal{D}}\Delta'\{\tilde{\phi}[\Delta]\tilde{\phi}[\Delta']\tilde{X}[\Delta]\tilde{X}[\Delta']\mathcal{G}_1(\Delta,\Delta';E)\} , \tag{2.19}$$

$\tilde{\phi}[\Delta]=\phi_0^0[\Delta+\Delta_f]$, $\tilde{X}[\Delta]=X_{01}[\Delta+\Delta_f]$, and $\mathcal{G}(\Delta,\Delta';E)$ is the momentum $P=0$ component of G:

$$\mathcal{G}_1(\Delta,\Delta';E)=\int_{-L/2}^{L/2}dY\,G_1(\Delta+\Delta_f,\Delta+\Delta_f^Y;E) . \tag{2.20}$$

Here, Δ_f^Y signifies the translated saddle-point configuration $\Delta_f^Y(x)=\Delta_f(x-Y)$. The imaginary part of the expression for $\mathcal{S}(\omega)$ in Eq. (2.18) can now be evaluated approximately by the method of steepest descents.

III. THE CLASSICAL DYNAMICS

In this section we first evaluate the ground-state wave function and the imaginary part of the lattice Green function S'' in the semiclassical approximation,[19,20] and then carry out the integrations over Δ and Δ' in Eq. (2.19) by the method of steepest descents. To do this we make extensive use of the PDX method. We will attempt to motivate these results with intuitive descriptions but have not actually derived them in the text; they are derived and discussed in detail in Refs. 15 and 19.

As we have already argued, the integrals in Eq. (2.19) are dominated by configurations near the saddle-point configuration Δ_f (which was named the "flip" by SK since it is the configuration at which the adiabatic potential flips from V_0 to V_1). Since Δ_f in turn closely resembles the soliton-pair configuration, $\Delta_{S\bar{S}}$, in Eq. (2.12) for soliton separation R determined by Eq. (2.14), we need only evaluate ϕ_0 and $\mathcal{G}_1''$ for configurations in the neighborhood of $\Delta_{S\bar{S}}(R_f)$. These configurations lie deep in the classically forbidden region of configuration space as shown in Fig. 4: The potential V_0 rises from zero to $2E_S$ as the soliton separation R increases from ξ_0 to several ξ_0, so $\tilde{\phi}[\Delta_{S\bar{S}}]$ is an exponentially decreasing function of R. The potential V_1 decreases as a function of R from $2\Delta_0$ to $2E_S$, so $\mathcal{G}_1''(\hbar\omega)$ is proportional to the penetration factor of a barrier of height $V_1-\hbar\omega$, and hence decreases exponentially with decreasing R. In the entire barrier region in the figure, $\xi_0<R<R_{+p}$, the overlap of ϕ_0 and $\mathcal{G}_1''$ is an exponentially small function of $1/h$. This justifies the use of the semiclassical approximation.

The problem of finding the ground-state wave function of a multidimensional potential well with a quadratic minimum is a standard problem which is discussed in Sec. IV and in Ref. 15,

$$\tilde{\phi}_0[\Delta]=\prod_k\left[\frac{\omega_k M}{\pi\hbar}\right]^{1/4}\exp[-W_0(\Delta_0,\Delta;0)/\hbar] , \tag{3.1a}$$

where $\{\omega_k\}$ are the harmonic phonon frequencies, and W_0 is the action of a classical path of energy 0 in the inverted potential, $-V_0$,

$$W_0(\Delta_0,\Delta;E)=\int_0^1 ds\sqrt{2M(s)\{V[\bar{\Delta}(s)]-E\}} . \tag{3.1b}$$

By classical path we mean simply a solution of the Euler-Lagrange equations. Here s parametrizes the classical path, $\bar{\Delta}(x,s)$, between the configurations $\bar{\Delta}(x;0)=\Delta_0$ and $\bar{\Delta}(x;1)=\Delta(x)$. $M(s)$ is the square of the length increment along the path (the "effective mass"):

$$M(s)=[M/(4\alpha)^2]\int dx\,a^{-1}\,|d\bar{\Delta}/ds|^2 . \tag{3.2}$$

Equation (3.1) would be exact if the lattice potential were perfectly harmonic (see, e.g., Appendix B of Ref. 15), and is the leading order term in $1/\hbar$ for an arbitrary potential.

Similarly, the leading order contribution to $\mathcal{G}_1''(\Delta,\Delta';E)$ for configurations Δ and Δ' deep in the classically forbidden region is given by

$$\mathcal{G}_1''(\Delta,\Delta',E)=\tfrac{1}{2}\Lambda(v[\Delta]v[\Delta'])^{-1/2} \times\exp\left[-\frac{1}{\hbar}\{W_1(\Delta,\Delta_{\rm tp}[\Delta],E) + W_1(\Delta',\Delta_{\rm tp}[\Delta'],E)\}\right] . \quad (3.3a)$$

Here,

$$W_1(\Delta,\Delta_{+p},E)=\int_1^2 ds\sqrt{2M(s)\{V[(s)]-E\}} , \quad (3.3b)$$

where for $1<s<2$ the path $\bar{\Delta}(s)$ is a classical path of energy $-E$ in the inverted potential $-V_1$ with energy $-E$ which satisfies the boundary conditions $\bar{\Delta}(1)=\Delta$ and $\bar{\Delta}(2)=\Delta_{\rm tp}[\Delta]$. $\Delta_{\rm tp}[\Delta]$ is a configuration on the hypersurface $\Sigma_{\rm tp}$ of turning points defined by

$$\Sigma_{\rm tp}=\{\Delta_{\rm tp}:V_1[\Delta_{\rm tp}]=E\} \quad (3.4)$$

for which $W_1(\Delta,\Delta_{\rm tp},E)$ is minimal, and so $\Delta_{\rm tp}$ is a functional of the end point Δ. $v(\Delta)$ is the magnitude of the classical velocity at the end point

$$v[\Delta]=\{(2/M)(V_1[\Delta]-E)\}^{1/2} . \quad (3.5)$$

Ω is a fluctuation determinant which measures the contribution from paths in the vicinity of the classical path, and is of order $\hbar^0$. We will discuss it in the next section. The factor of $\frac{1}{2}$ in Eq. (3.3) is found by connecting $\mathcal{G}_1''$ to outgoing plane waves in the allowed region using the Airy function connection formula. (In the bounce formalism it is obtained from the Gaussian integration over half a saddle point in path space.[12])

Since $\mathcal{G}_1''$ asymptotically factorizes (for Δ and Δ' deep under the barrier), we can carry out the two integrations in Eq. (2.19) independently. They are dominated by the saddle-point configuration, which we call the "flip" Δ_f since it is the configuration at which the transition from state $j=0$ to $j=1$ occurs. It is found by maximizing $\tilde{\phi}_0$ and $\mathcal{G}_1''$ simultaneously:

$$\frac{\delta}{\delta\Delta(x)}[W_0(\Delta_0,\Delta;0)+W_1(\Delta,\Delta_{+p};\hbar\omega)]=0 . \quad (3.6)$$

Since the derivative of the action with respect to its end point is the classical momentum, Eq. (3.6) has the simple interpretation that the momentum is continuous at the flip. This further implies that the flip configuration must lie on the hypersurface defined by

$$\Sigma_f=\{\Delta_f:V_0[\Delta_f]=V_1[\Delta_f]-\hbar\omega\} . \quad (3.7)$$

We can therefore conclude that the exponential contribution to $\mathcal{G}''(\omega)$ is determined by a single continuous and smooth classical path called the instanton path Δ_I, which minimizes the action of a round trip ("bounce") in configuration space from Δ_0 to the turning point surface $\Sigma_{\rm tp}$ and back, yielding

$$S''(\omega)\sim\exp(-W/\hbar) \quad (3.8a)$$

and

$$W=2\int_0^2 ds\sqrt{2M(s)V(s,\omega)} , \quad (3.8b)$$

where M is the effective mass [Eq. (3.2)], and V is the "unified" potential

$$V(s,\omega)=V(\Delta_I(s),\omega)=\min(V_0,V_1-\hbar\omega) . \quad (3.9)$$

$\Delta_I(s)$ is equal to Δ_f as it crosses Σ_f: $\Delta_I(1)=\Delta_{S\bar{S}}(R_{\rm tp})=\Delta_f$.

Let us now consider the family of soliton pair configurations $\Delta_{S\bar{S}}(R,K,A)$ defined in Eq. (2.12). SK asserted that the instanton path lies close to the adiabatic path in which the soliton width, $K(R)$, and amplitude, $A(R)$, are determined as a function the soliton separation R as in Eq. (2.13). Conveniently, exact analytic expressions[21] for the potentials V_0 and V_1 are known for these configurations:

$$V_0(R)=(4/\pi)\{\tanh(KR)-\tan^{-1}[\sinh(KR)]\,\mathrm{sech}(KR)\} ,$$
$$V_1(R)=V_0(R)+2\Delta_0\,\mathrm{sech}(KR) . \quad (3.10)$$

Here we support their statement by a time-scales argument and a variational computation. As stated previously, the configurations $\Delta_{S\bar{S}}$ minimize V for a fixed value of the electronic level spacing $\epsilon_1-\epsilon_0$. The spectrum of small amplitude (phonon) excitations around $\Delta_{S\bar{S}}$ has been extensively studied for $R=\xi_0[\Delta_{S\bar{S}}(x)=\Delta_0]$, $R\gg\xi_0$ (two far-separated solitons), and $R=\sinh^{-1}(1)/\sqrt{2}$ (the polaron). It was found that the continuum of optical phonons always has a lower cutoff at $\hbar\omega_0$. The characteristic time scale of motion along the R coordinate can be crudely estimated as

$$\tau=\langle(d^2V/dR^2)[1/M(R)]\rangle\sim\omega_0^{-1} . \quad (3.11)$$

Since motion along the instanton path is thus slow compared to the typical continuum phonon frequencies, these modes are adiabatic slaves to the R motion. The true instanton path can only differ significantly from $\Delta_{S\bar{S}}$ by a modification of its shape, represented by the softer localized modes parametrized by the collective coordinates K and A. We have numerically determined the values of $K(R)$ and $A(R)$ which minimize the action using Jacobi's form of the least-action principle,[22]

$$W[\Delta_I]=\min(W[\Delta]) . \quad (3.12)$$

We therefore minimize the action with respect to the family of soliton-pair configurations given by Eq. (2.12). We parametrized the path by the soliton-pair separation $R=R(s)$, and choose $K(R)$ and $A(R)$ so as to minimize W. We found that $K(R)$ and $A(R)$ are within 10% of their adiabatic values, Eq. (2.13), and that the instanton action is within 1% of the action along the adiabatic path. This conclusively verifies the ansatz of SK and allows us to parametrize the instanton path in this way.

In Fig. 2 we plot the contours of the potential V in the two-dimensional parameter space of K and R (A is set equal to K). It illustrates the tunneling problem as finding the minimum action path between the line $K=0$ and the surface Σ_{+p}. The vector δ_K parametrizes the symmetric shape oscillation mode $u_S(x)$ which is a normal mode of the lattice at large separations. Since the tunneling coordinate is coupled to this mode, as suggested by the

potential contours plotted in Fig. 2, we expect this mode to be excited by phonon emission simultaneously to the motion of the instanton path. In Fig. 3 the instanton configurations are drawn. Also shown is the form of the breathing mode on the pair of far-separated solitons. In Fig. 4 the potentials [Eqs. (3.10)] are drawn as solid lines.

IV. QUANTUM CORRECTIONS, *e-e* INTERACTIONS, AND THE PREFACTOR

Until now we have focused only on the instanton path. The prefactors of $\tilde{\phi}_0$ and $\mathscr{G}_1''$ in Eqs. (3.1) and (3.3) are a measure of how many paths there are "near" the classical path in the sense that their action is nearly the same. Likewise, the Gaussian approximation to the integral in Eq. (2.19) over configurations at which the electronic transition occurs measures how many classical paths have action near that of the instanton path. To calculate the prefactor of S'' we must account for all these factors. To do this, we expand the action functional to second order in the deviation from the instanton path $\delta\Delta(s) = \Delta(s) - \Delta_I(s)$. The sum over paths can then be evaluated formally since the path integral is quadratic. However, the resulting fluctuation determinant is usually rather dif-

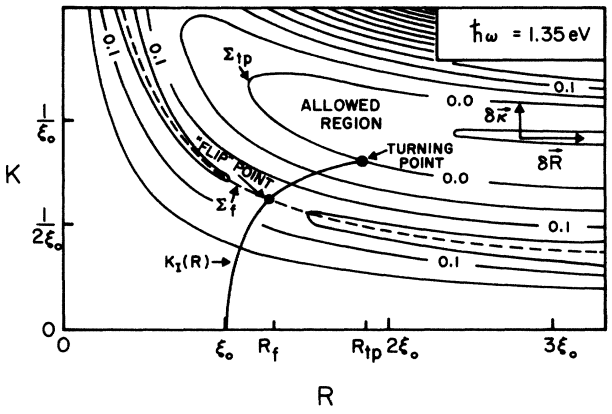

FIG. 2. Potential V of Eq. (3.9) for soliton-pair configurations given by Eq. (3.10) with A set equal to K. The ground state lies on the two axis. Σ_{tp} and Σ_f are defined in Eqs. (3.4) and (3.7), respectively. The instanton path is parametrized by $K_I(R)$. δK denotes the direction of the symmetric width oscillation mode $u_S(x)$.

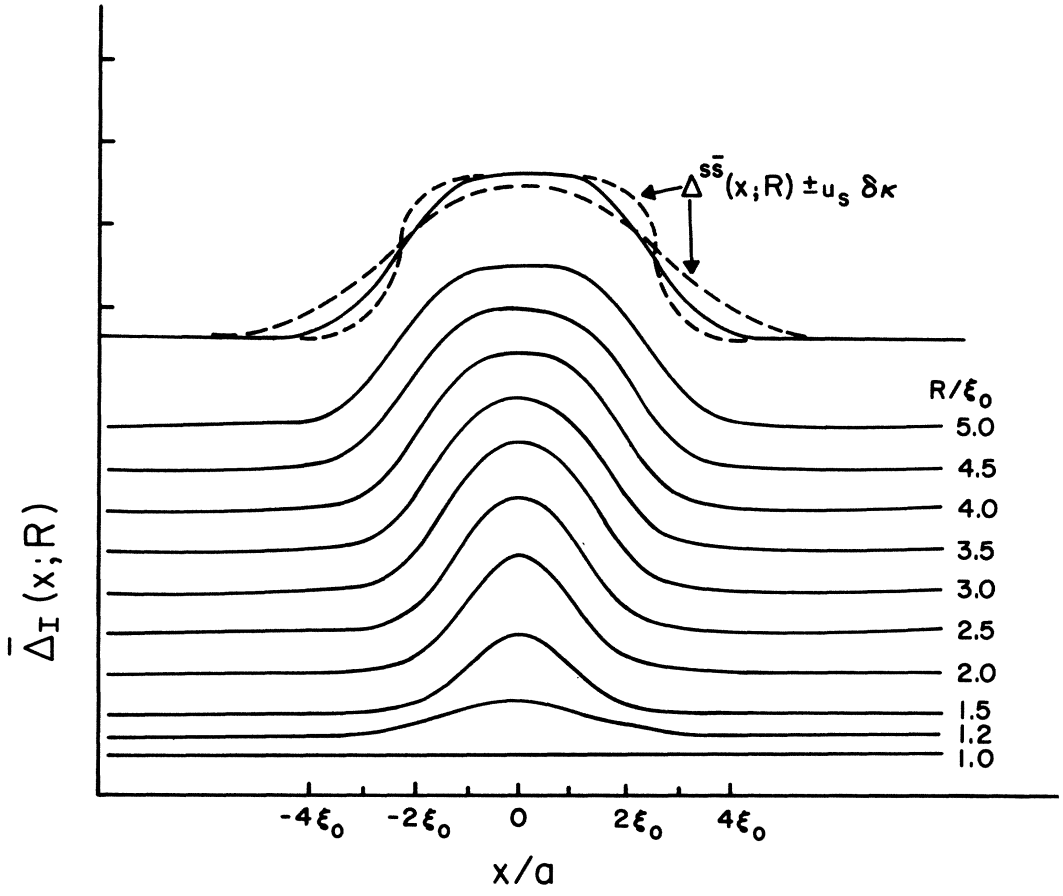

FIG. 3. Instanton path [as given by Eqs. (2.12) and (2.13)] at different values of R. The bottom configuration is the ground state, and the top one describes a far-separated soliton pair with a symmetric width mode u_S drawn as dashed lines.

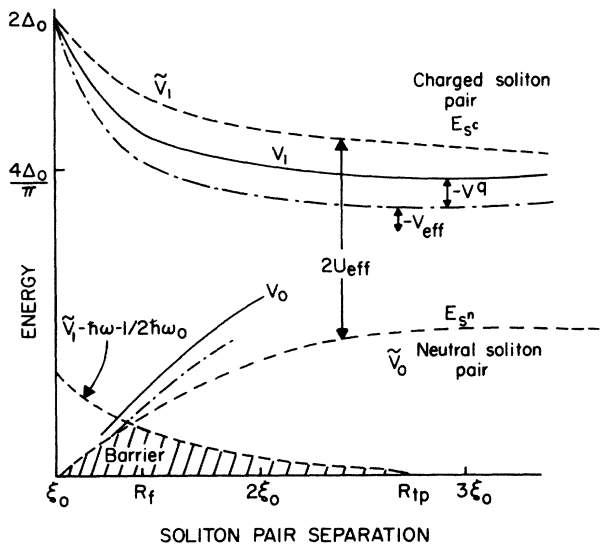

FIG. 4. Bare and dressed potential energies along the instanton path [Eq. (3.10) and (4.9), respectively], and the tunneling barrier for photon energy $\hbar\omega$. Solid lines: the bare potentials Eq. (3.10); dashed-dotted lines: the renormalized energies including the quantum corrections [Eq. (4.3)]; dashed lines: the dressed potential energies including the effects of e-e interactions. In this figure we chose $U_{\rm eff}=0.4\Delta_0$ and $V_{\rm eff}=-0.12\Delta_0$.

ficult to evaluate since it is formally equivalent to evaluating the propagator of a continuum of harmonic phonons with a time-dependent dynamical matrix $D(x,x';R(t))$,

$$D(x,x';R)=\frac{\delta^2}{\delta\Delta(x)\delta\Delta(x')}V[\Delta]\,|_{\Delta=\Delta_{S\bar{S}}(R)}\ , \tag{4.1}$$

where $j=0$ for $s<1$ and $j=1$ for $s>1$. Fortunately, as we stressed previously, the motion along the instanton path is slow compared to the characteristic phonon frequency. This allows us to evaluate the prefactors using the adiabatic fluctuations approximation (discussed in detail in Refs. 15 and 19) which amounts to an adiabatic approximation for the phonon propagator. We define the instantaneous eigenmodes of the dynamical matrix

$$\int dx' D(x,x';s)u_k(x';s)=(1/g^2)\omega_k^2(s)u_k(x;s)\ . \tag{4.2}$$

There are two special modes: u_0 is the translation mode we encountered previously and u_1 is the mode parallel to the instanton path $u_1(x)\alpha d\Delta_I/dR$. When we sum over fluctuations in Eq. (2.19), we sum over the amplitude of all transverse modes, that is all modes which are perpendicular to both u_0 and u_1. In the adiabatic approximation, the transverse modes simply remain in their instantaneous ground state as the system tunnels. Thus, the effects of quantum fluctuations are as follows: (1) There is a quantum renormalization of the bare potential V_j in Eqs. (3.9) and (3.10) due to the shift in the phonon frequencies along the instanton path

$$\bar{V}_j(R)=V_j(R)+\tfrac{1}{2}\hbar\Omega(R)-\delta_{j1}\tfrac{1}{2}\hbar\omega_0\ , \tag{4.3a}$$

$$\Omega(R)=\sum_k{}'\{\omega_k(R)-\omega_k\}\ , \tag{4.3b}$$

where $\{\omega_k(R)\}$ are the transverse phonon frequencies relative to the lattice configuration $\Delta_I(R)$, $\{\omega_k\}$ are the phonon frequencies of the perfectly dimerized lattice ($R=\xi_0$), and the prime denotes sum over all modes excluding $k=0$ and 1. (2) There are two prefactors, the ground-state normalization in Eq. (3.1a) and the factor in Eq. (3.3a), which measure the cross-sectional area of the bundle of the important path. We return to this below.

The phonon spectrum, and in particular the spectral sums in Eq. (4.3b) have been evaluated for $R=\xi_0$ and $R\to\infty$ (free solitons) by Nakahara and Maki.[23] The polaron spectrum sum at $R=R_P=\xi_0\ln(1+\sqrt{2})/\sqrt{2}$ has been computed by Hicks and Blaisdell.[9] To obtain values for Ω, we must subtract the contributions of the two special modes from their results which yields

$$\Omega/\omega_0=\begin{cases}0.00 & \text{for } R=\xi_0\ ,\\ -0.20 & \text{for } R=R_P\ ,\\ -0.22 & \text{for } R\to\infty\ .\end{cases} \tag{4.4}$$

To obtain an expression for $\Omega(R)$ at intermediate R we use the simple interpolation scheme:

$$\Omega(R)/\omega_0=-0.22(4\pi/\Delta_0)^{-1}V_0(R)\ . \tag{4.5}$$

The small and negative values of $\Omega(R)$ reflects the fact that the only major change in the phonon spectrum due to the presence of the solitons is the appearance of four localized modes: the two modes u_0 and u_1 which derive from the soliton translation mode and do not contribute to Ω, and the symmetric and antisymmetric combination of the soliton width modes $\bar{u}_S$ and u_S, respectively. The rearrangement of the continuum modes does not make much of a contribution to Ω.

Finally, we are ready to evaluate $\mathscr{G}''$. The adiabatic fluctuations approximation (AFA) allows us to express the integral over fluctuations about the classical path in terms of the $N-2$ transverse phonon modes which span Σ_f [$u_k(x,R)$ for $k>2$ defined in Eq. (4.2)] and one mode normal to Σ_f. It is therefore convenient to express the measure for the integral in Eq. (2.19) as

$$\tilde{\mathscr{D}}\Delta=\prod_k{}'da_k[M(R_+)/M]^{1/2}dR\ , \tag{4.6}$$

where a_k is the amplitude of the k adiabatic phonon, and $M(R_f)/M$, defined in Eq. (3.2), is the Jacobian of the transformation. The transverse integrals are now trivial. We found in Eq. (3.3a) that in the semiclassical limit, $\mathscr{G}''$ factorizes into a product of Δ- and Δ'-dependent pieces. The AFA allows us to write the prefactor Ω as the product of the $N-2$ transverse phonon normalization factors. Thus, the integral over transverse fluctuations is unity due to the normalization of the wave functions. The R integral is a simple integral over the Gaussian factor $\exp[-\frac{1}{2}A(R-R_f)^2]$ where

$$A=\frac{1}{\hbar}\frac{d^2}{dR^2}(W_0+W_1)\,|_{R=R_f}$$
$$=\frac{1}{\hbar}\left[\frac{M(R)}{2V(R)}\right]^{1/2}\frac{d}{dR}(V_0-V_1)\,|_{R=R_f}\ .$$

The result is

$$\mathcal{S}''(\omega)=[2M(R_f)\omega_0/\hbar][A]^{-1}\,|\,\tilde{X}(R_f)\,|^2\exp(-W/h)\,, \tag{4.7}$$

where W is the instanton action given in Eq. (3.8).

Let us now examine the validity of the AFA. It is valid so long as $\omega_k\tau$ are large, where ω_k is the characteristic time scale for motion along the instanton path defined in Eq. (3.11). All the continuum modes satisfy this condition fairly well; these modes are not usually excited during photoproduction of solitons. However, for the soliton shape modes, $\omega_S\tau\approx 1$, there is a substantial probability that the solitons will be produced in an internally excited state. This claim is substantiated by the observation that the instanton path bends strongly in the two-dimensional parameter space of the collective coordinates K and R as demonstrated in Fig. 2. In the oversimplified picture of 2D tunneling represented by the potential $V(R,K)$, the strong overlap of excited states in the K direction with the transverse adiabatic phonon would yield a large branching ratio for producing solitons in internally excited states. the real problem is somewhat more complicated since the effective mass also depends on R and K. However, this does not change the conclusion qualitatively.

Until now we have ignored the effects of electron-electron interactions. We now proceed to discuss how our results are modified when these interactions are included. Wu and Kivelson[16] (WK) have studied the TLM model with weak e-e interactions and calculated the corrections, or "dressing," of the various bare quantities such as the ground-state dimerization and physical gap. These effects are automatically included in our calculation by using the experimentally measured gap energy. More importantly, the interactions alter the form of the adiabatic lattice potential by altering the electronic energies of the states $j=0$ and 1. (Note, although in the presence of interactions, the states 0 and 1 need not have a simple interpretation in terms of the occupancies of one-electron states, they can still be defined as the two lowest-energy singlet electronic states.) WK showed that interactions change the soliton creation energies and, in particular, lift the degeneracy between the neutral and charged soliton creation energies E_{S^n} and E_{S^c}, respectively. We define effective interaction parameters (which can be evaluated perturbatively in terms of the bare interactions):

$$U_{\rm eff}=\tfrac{1}{2}(E_{S^c}-E_{S^n}) \tag{4.8a}$$

and

$$V_{\rm eff}=\tfrac{1}{2}(E_{S^c}+E_{S^n})-E_S\,, \tag{4.8b}$$

where in Eq. (4.9b) E_S is the soliton creation energy in the absence of interactions. WK have also shown that the soliton equilibrium widths ξ_n and ξ_c differ from the noninteracting value ξ_0 such that $\xi_n<\xi_0<\xi_c$. From these results we can determine the effect of interactions on the lattice potential in the asymptotic region $R\gg\xi_0$. Again we use the same simple interpolation formula to express the effect of interactions on the dressed lattice potential $\tilde{V}_j(R)$ for intermediate R [$\bar{V}$ is defined in Eq. (4.3)]:

$$\tilde{V}_j(R)=\bar{V}_j(R\lambda_j)+U_j(R\lambda_j)\,, \tag{4.9a}$$

$$U_0(R)=[V_0(R)/2E_S](V_{\rm eff}-U_{\rm eff})\,, \tag{4.9b}$$

$$U_1(R)=\{[2\Delta_0-V_1(R)]/(2\Delta_0-2E_S)\}(V_{\rm eff}+U_{\rm eff})\,, \tag{4.9c}$$

and λ_j is the e-e interaction-induced scale change: $\lambda_0=\xi_n/\xi_0$ and $\lambda_1=\xi_c/\xi_0$. All previous calculations can then be corrected by replacing $V_j(R)$ by $\tilde{V}_j(R)$ wherever it appears. In Fig. 4 the bare and dressed potentials are plotted.

V. RESULTS AND DISCUSSION

To compare our results with experiment, we use the best estimates available to us of the various parameters[24,25] (see discussion in Ref. 2): $t_0=2.5$ eV, $2\Delta_0=1.65$ eV, and $\omega_0=1400\ {\rm cm}^{-1}$. The density n of the fibril structure is $0.012a$ where $a=1.1$ Å. The value of $U_{\rm eff}$ was estimated by WK to be 0.22 eV based on measurements of the spin density of a neutral soliton, and ξ_n/ξ is approximately 0.8. However, the value of $V_{\rm eff}$ is unknown. We therefore plot Eq. (4.19) using two estimates of $V_{\rm eff}$: 0.0 eV and -0.2 eV, as solid and dashed lines, respectively. The energy range goes up to 1.5 eV, since for higher energies both the semiclassical approximation and the Born-Oppenheimer approximation break down.

The data of Blanchet *et al.* is plotted as open circles. The data of Weinberger *et al.* is marked by ○ and by × for the pristine and NH-compensated samples, respectively. The latter data shows a markedly different exponential tail which we attribute to the high impurity concentration. The solid circles are photoinduced absorption data of Blanchet *et al.* at 1370 $\rm cm^{-1}$ plotted in arbitrary units. Here the slower dependence at higher energies suggests that the branching ratio of the electron hole decay rate into stable solitons decreases with energy. Figure 1 demonstrates the agreement of our calculation with the absolute magnitude and behavior of the absorption coefficient in the tail region where $V_{\rm eff}$ is our only free parameter. Cleaner samples and higher sensitivity measurements of this region would enable us to obtain a more accurate value for $V_{\rm eff}$.

The expression for $\mathcal{S}''$ in Eq. (4.7) derives its ω dependence primarily from the ω dependence of the instanton action W. We have computed W numerically; however, it can be crudely approximated by replacing the true potential barrier with similar triangles in the energy range 1.2–1.5 eV. This yields the following form for $\ln[\alpha(\omega)]$:

$$\ln[\alpha(\omega)]\approx-[(\hbar\omega-2\tilde{\Delta}_0)/\tilde{\Delta}_1]^{3/2}+12.3\ln({\rm cm}^{-1})\,, \tag{5.1}$$

where, for example, $2\tilde{\Delta}_0=1.62$ eV and $\tilde{\Delta}_1=0.079$ eV, for the value of $V_{\rm eff}=0.0$ eV. (It differs from the quadratic power-law result of Su and Yu.[13] Coincidently, it has the functional form of the density of states in a one-dimensional disordered model,[7] although its energy scale is much smaller than Δ_1, which was derived in the Introduction.

A critical test of the model could be obtained by measuring the isotope dependence of $\alpha(\omega)$ in pristine

trans-$(CD)_x$: The values of $2\Delta_0$ and the threshold depend (up to small quantum corrections) on t_0 and K and are therefore approximately mass independent. Since $\hbar\omega_0 \propto M^{-1/2}$ the mass dependence of α is given by

$$\alpha(\omega,M) \approx \left[\frac{M}{M_{CH}}\right]^{1/2} \exp\left[-\frac{1}{\hbar}\left[\frac{M}{M_{CH}}\right]^{1/2} W\left[\frac{\hbar\omega}{\Delta_0}\right]\right] . \tag{5.2}$$

The isotope dependence would be completely different if the absorption tail were due to strong electron correlations or static disorder.

As mentioned earlier, soliton-pair generation is accompanied by excitations of the shape modes. The Raman active localized mode of $\hbar\omega_2 \approx 0.16$ eV was attributed to the width oscillation of a single soliton. We thus expect that in the low-energy (tail) regime the absorption curve should have small- amplitude ripples with a periodicity of $\hbar\omega_2$. In systems in which the ground-state degeneracy is lifted, such as in *cis*-$(CH)_x$, or in *trans*-$(CH)_x$ with strong interchain interactions, one expects the final soliton pairs to be confined by a potential that increases with the separation R. However, the final-state structure due to the quantized periodic motion of the breathing mode would correspond to level spacings of order 10^{-2} eV, and thus we do not expect them to be observable in the absorption curve.

Note added in proof. H. Schaffer and A. J. Heeger, of University of California, Santa Barbara, have recently observed isotope dependent shifts in the sub-gap absorption of *trans*-$(CH)_x$ versus *trans*-$(CD)_x$. We thank them for the communication of their data prior to publication.

ACKNOWLEDGMENTS

This work was partially supported by the National Science Foundation Grant No. DMR-83-18051. S.K. was partially supported by the Alfred P. Sloan Foundation.

*Present address: James Franck Institute, University of Chicago, Chicago, IL 60637.

[1]W. P. Su, J. R. Schrieffer, and A. J. Heeger, Phys. Rev. B **22**, 2099 (1980), **28**, 1138(E) (1983).
[2]S. Kivelson, in *Solitons,* edited by S. Trullinger and V. Zakharov (North-Holland, Amsterdam, 1986).
[3]T. K. Lee and S. Kivelson, Phys. Rev. B **29**, 6687 (1984).
[4]B. R. Weinberger *et al.*, Phys. Rev. Lett. **53**, 86 (1984).
[5]G. B. Blanchet *et al.*, Phys. Rev. Lett. **51**, 2132 (1983).
[6]L. Lauchlan *et al.*, Phys. Rev. B **24**, 3701 (1981).
[7]B. I. Halperin, Phys. Rev. **139**, A104 (1965); J. Zittartz and J. S. Langer, *ibid.* **148**, 741 (1966).
[8]H. Takayama, Y. R. Lin-Liu, and K. Maki, Phys. Rev. B **21**, 2388 (1980).
[9]J. C. Hicks and G. A. Blaisdell, Phys. Rev. B **31**, 919 (1985).
[10]A similar discussion was also given by S. A. Brazovskii and I. E. Dzyaloshinski, Z. Eksp. Teor. Fiz. **71**, 2338 (1976) [Sov. Phys.—JETP **44**, 1233 (1976)].
[11]J. P. Sethna and S. Kivelson, Phys. Rev. B **26**, 3513 (1982).
[12]C. G. Callan, Jr. and S. Coleman, Phys. Rev. D **16**, 1762 (1977); S. Coleman, *The Whys of Subnuclear Physics,* edited by A. Zichichi (Plenum, New York, 1979).
[13]Z. B. Su and Lu Yu, Phys. Rev. B **27**, 5199 (1983).
[14]A. Auerbach, S. Kivelson, and D. Nicole, Phys. Rev. Lett. **53**, 411 (1984).
[15]A. Auerbach and S. Kivelson, Nucl. Phys. **B257[F14]**, 799 (1985).
[16]W.-K. Wu and S. Kivelson, Phys. Rev. B (to be published); S. Kivelson, H. B. Thacher, and W.-K. Wu, Phys. Rev. B **31**, 3785 (1985); S. Kivelson and W.-K. Wu, Mol. Cryst. Liq. Cryst. **118**, 9 (1985).
[17]N. Suzuki *et al.*, Phys. Rev. Lett. **45**, 1209 (1980).
[18]D. Campbel (private communication).
[19]P. van-Baal and A. Auerbach, Nucl. Phys. B (to be published).
[20]R. Dashen, B. Hasslacher, and A. Neveu, Phys. Rev. D **10**, 4114 (1974).
[21]A. Bishop and D. Campbel, Nucl. Phys. **B200**, 297 (1982).
[22]H. Goldstein, *Classical Mechanics* (Addison-Wesley, Reading, Mass., 1980), Sec. 8-6.
[23]M. Nakahara and K. Maki, Phys. Rev. B **25**, 7789 (1982).
[24]We use the same values of t_0 and $2\Delta_0$ as in Ref. 10, but we choose $\hbar\omega_0$ as the optical band edge measured by C. R. Fincher *et al.*, Phys. Rev. B **19**, 4140 (1979). Thus the quantity $S_0=(\Delta_0/2\alpha\hbar)(2t_0M)^{1/2}=7.59$, which differs appreciably from the estimate $S_0=13$ of SK. Other estimates of Δ_0 and $\hbar\omega_0$, such as in Refs. 8 and 21, further decrease the value of S_0 and proportionally the first term in Eq. (5.1).
[25]Z. Vardeny *et al.*, Phys. Rev. Lett. **51**, 2326 (1983).